



Free convective heat and mass transfer of magnetic bio-convective flow caused by a rotating cone and plate in the presence of nonlinear thermal radiation and cross diffusion

M. Ganeswara Reddy^{a,*}, and N. Sandeep^b

^aDepartment of Mathematics, Acharya Nagarjuna University Campus, Ongole, 523 001, India

^bDepartment of Mathematics, VIT University, Vellore),632 014, India

Article info:

Received: 23/04/2016

Accepted: 18/01/2017

Online: 15/07/2017

Keywords:

MHD,
Nonlinear thermal radiation,
Cross diffusion,
Gyrotactic microorganisms,
Rotating cone and plate,
Free convection.

Abstract

This article explores the heat and mass transfer behavior of magnetohydrodynamic free convective flow past a permeable vertical rotating cone and a plate filled with gyrotactic microorganisms in the presence of nonlinear thermal radiation, thermodiffusion, and diffusion thermo effects. Dual solutions are presented for the flow over a rotating cone and a rotating flat plate cases. Similarity variables are employed to convert the nonlinear partial differential equations into ordinary differential equations. Comparisons with previously published work are performed and results are found to be in excellent agreement. The resultant non-dimensional governing equations along with associated boundary conditions are solved numerically using Runge–Kutta and Newton’s methods. The impact of pertinent parameters on velocity, temperature, concentration and density of the motile microorganisms along with the friction factor, local Nusselt, Sherwood numbers, and the local density of the motile microorganisms is determined and analyzed with the help of graphs and tables. Results prove that there is a significant variation of heat and mass transfer in the flow over a rotating cone and a plate. It is also found that the heat and mass transfer performance of the flow over a rotating cone is significantly high when compared with the flow over a rotating plate.

1. Introduction

Convective heat transfer with thermal radiation effects become intensified at high absolute temperature levels due to the basic difference between the radiation, convection, and conduction energyexchange mechanisms. In the context of space technology, some devices for

space applications are designed to operate at high-temperature levels in order to achieve high thermal efficiency. Hence, the effects of radiation have vital importance when calculating thermal effects in the processes involving the high temperatures, engineering processes

* Corresponding author
email address: mgrmaths@gmail.com

including thermal energy storage, gas turbines, nuclear turbines, die forging and chemical reactions. By keeping this into view, Aboeldahab [1] studied the thermal radiation effect on heat transfer in an electrically conducting fluid past a stretching surface. The thermal radiation boundary-layer flow of a nanofluid past a stretching sheet under the applied magnetic field was analyzed by Gnaneswara Reddy [2]. Abo-Eldahab and Elgendy [3] presented a radiation effect on convective heat transfer in an electrically conducting fluid at a stretching surface with variable viscosity and uniform free stream. Further, Aziz [4] numerically investigated the viscous flow over a flat plate with convective boundary conditions.

Radiation effects in the Blasius and Sakiadis flows with convective boundary conditions have been described by Cortell [5]. Ishak [6] provided the numerical solution for the flow and heat transfer over a permeable stretching sheet with convective boundary conditions. Yao et al. [7] obtained a closed-form exact solution for viscous flow over a permeable stretching/shrinking convectively heated wall. Alsaedi et al. [8] computed exact solutions for a steady flow of Jeffrey fluid over a linearly stretching surface with convective boundary conditions. Makinde and Aziz [9] considered the analysis of convective heat transfer in the steady flow of a nanofluid. Recently, Gnaneswara Reddy [10] emphasized the thermal radiation and chemical reaction effects on MHD mixed convective boundary layer slip flow in a porous medium with a heat source and Ohmic heating. The influence of thermophoresis, viscous dissipation, and joule heating on steady MHD flow over an inclined radiative isothermal permeable surface was studied by Gnaneswara Reddy [11].

The impact of combined heat and mass transfer from different geometries embedded in porous media has many engineering and geophysical applications such as the extraction of geothermal energy, drying of porous solids, food processing and storage, thermal insulation of buildings, enhanced oil recovery, nuclear power plants, and cooling system of electronic devices. A comprehensive account of the fundamental

theoretical and experimental works is provided in the recent books Bejan [12], Bejan and Khair [13], Neild and Bejan [14], Pop and Ingham [15] and Ingham and Pop [16]. Also, the investigation of heat and mass transfer over rotating bodies is of considerable importance due to its applications in various areas of geophysics, technologies and engineering. Such an investigation is important in the design of turbines and turbo-machines, in estimating the flight path of rotating wheels and spin stabilized missiles and in the modeling of many geophysical vortices. In view of this, Sparrow and Gregg [17] analyzed theoretically the problem of laminar heat transfer from a rotating disk with suction effect. Hering and Grosh [18] analyzed the problem of laminar natural convection from a non-isothermal cone. Kreith [19] presented the problem of convective heat transfer systems from various types of axisymmetric bodies. The buoyancy-induced flow and temperature fields around a vertical rotating cone are studied analytically by Himasekhar et al. [20]. Chamkha [21] considered the hydromagnetic combined convection of power-law fluid along isothermal rotating cone or disks embedded in a porous medium. Takhar et al. [22] studied the unsteady mixed convection flow over a vertical cone rotating in an ambient fluid with a time-dependent angular velocity. Roy and Anilkumar [23] illustrated the heat and mass transfer of unsteady mixed convection flow of a rotating cone in a rotating fluid. Gnaneswara Reddy and Bhaskar Reddy [24] presented the mass transfer and heat generation effects on MHD flow past an inclined vertical surface in a porous medium. Bhuvanavijaya and Mallikarjuna [25] investigated the effect of variable thermal conductivity on convective heat and mass transfer over a vertical plate in a rotating system with variable porosity regime. Lie group analysis of heat and mass transfer effects on steady MHD free convection dissipative fluid flow past an inclined porous surface with heat generation was studied by Gnaneswara Reddy [26]. Recently, the chemical reaction effects on MHD convective heat and mass transfer on the flow past a rotating vertical cone was studied by Mallikarjuna et al. [27]. Awad et al. [28] studied

the diffusion thermo and Awad et al. [28] have been studied the diffusion thermo and thermo diffusion effects on the flow through an inverted cone in a porous medium. Dual solutions for analyzing the heat and mass transfer characteristics of non-Newtonian nanofluid over a stretching sheet in a porous medium have been recently analyzed by Sandeep et al. [29]. Raju and Sandeep [30] investigated the heat and mass transfer in magnetic non-Newtonian bio-convection flow over a rotating cone/plate with cross-diffusion. Cross diffusion effects in hydromagnetic thermal radiative Carreau fluid has been studied by Gnanaswara Reddy and Sandeep [31].

Due to numerous applications in the energy-exchange mechanisms and to design of turbines and turbo-machines, estimating the flight path of rotating wheels and spin stabilized missiles and in the modeling of various geophysical vortices. In this study, the authors make an attempt to propose a mathematical model to explore the characteristics of the magnetohydrodynamic free convective heat and mass transfer of the flow past a permeable vertical rotating cone and plate filled with gyrotactic microorganisms in the presence of nonlinear thermal radiation, thermo diffusion, and diffusion thermo effects.

2. Formulation of the problem

A two-dimensional, steady, laminar and incompressible boundary layer flow of a radiating fluid induced by a vertical rotating cone and plate in a porous medium with convective surface boundary conditions is considered. Here the cone and plate rotate with an angular velocity Ω and a variable porous medium as shown in Fig.1. A magnetic field of strength B_0 is applied along Z -direction. The induced magnetic field is neglected upon the assumption of small magnetic Reynolds number. Crossdiffusion effects are taken into account. Further, it is assumed that the cone and plate are made with a non-conducting material. Under the usual boundary layer assumptions, the governing equations are obtained as reported by Mallikarjuna et al. [27].

2.1. Flow analysis

$$\frac{\partial(r^h xu)}{\partial x} + \frac{\partial(r^h xw)}{\partial z} = 0, \tag{1}$$

$$\begin{aligned} & \delta^{-2} \rho \left(u \frac{\partial u}{\partial x} + w \frac{\partial u}{\partial z} - \frac{v^2}{x} \right) - \delta^{-1} \mu \frac{\partial^2 u}{\partial z^2} \\ & = \rho g_e (\beta_T (T - T_\infty) + \beta_C (C - C_\infty)) \cos \alpha - \frac{\mu}{K} u - \sigma B_0^2 u, \end{aligned} \tag{2}$$

$$\begin{aligned} & \delta^{-2} \rho \left(u \frac{\partial v}{\partial x} + w \frac{\partial v}{\partial z} + \frac{uv}{x} \right) - \delta^{-1} \mu \frac{\partial^2 v}{\partial z^2} \\ & = -\frac{\mu}{K} v - \sigma B_0^2 v, \end{aligned} \tag{3}$$

with the boundary conditions:

$$\left. \begin{aligned} u = 0, \quad v = r\Omega, \quad w = 0, \quad \text{at } z = 0, \\ u = 0, \quad v = 0, \quad \text{as } z \rightarrow \infty, \end{aligned} \right\} \tag{4}$$

where h is a positive constant, ρ is the fluid density, δ is the porosity parameter, μ is the dynamic viscosity, g_e is the acceleration due to gravity, β_T and β_C are the volumetric expansions due to temperature and concentration differences, respectively, σ is the electrical conductivity, α is the cone half angle, and K is the permeability of porous medium.

Here $h = 1$ denotes the flow over a vertical rotating cone and $h = \alpha = 0$ represents the flow over a vertical rotating plate.

Setting the following non-dimensional variables:

$$\left. \begin{aligned} \eta = v^{-1/2} (\Omega \sin \alpha)^{1/2} z, u = x \Omega \sin \alpha f(\eta), \\ v = x \Omega \sin \alpha g(\eta), r = x \sin \alpha, w = (v \Omega \sin \alpha)^{1/2} h(\eta), \\ \theta(\eta) = \frac{T - T_\infty}{T_w - T_\infty} \text{ (or) } T = T_\infty (1 + (\theta_w - 1)\theta), \\ \phi(\eta) = \frac{C - C_\infty}{C_w - C_\infty}, \xi(\eta) = \frac{N - N_\infty}{N_w - N_\infty}, \\ T_w(x) - T_\infty = \frac{(T_L - T_\infty)x}{L}, \\ C_w(x) - C_\infty = \frac{(C_L - C_\infty)x}{L}, N_w(x) - N_\infty = \frac{(N_L - N_\infty)x}{L}, \end{aligned} \right\} \tag{5}$$

Here L and T_L correspond to the slant height and surface temperature of the cone, respectively and C_L is the cone surface concentration at the base ($x = L$). Using Eq. (5), the Eqs. (1) to (3) are transformed to:

$$f = -\frac{1}{2}h', \tag{6}$$

$$-\delta^{-1}h''' + \delta^{-2}hh'' + (M + Da^{-1})h' + \delta^{-2}\left(-\frac{1}{2}h'^2 + 2g^2\right) + 2\Lambda(\theta + \Gamma\phi)\cos\alpha = 0, \tag{7}$$

$$-\delta^{-1}g'' - \delta^{-2}(hg' - h'g) - (M + Da^{-1})g = 0, \tag{8}$$

with the transformed boundary conditions:

$$\left. \begin{aligned} h' = 0, g = 1, & \quad \text{at } \eta = 0, \\ h' = 0, g = 0, & \quad \text{as } \eta \rightarrow \infty, \end{aligned} \right\} \tag{9}$$

where M is the dimensionless magnetic parameter, Ha^2 is the Hartmann number, Da^{-1} is the inverse of Darcy number, Gr_L is the Grashof number, Re_L is the Reynolds number, Λ is the dimensionless buoyancy parameter; $\Gamma < 0$ corresponds to opposing flow while $\Gamma > 0$ corresponds to aiding flow; and M is the magnetic parameter, which are given by:

$$Da^{-1} = \frac{\nu}{K\Omega\sin\alpha}, M = \frac{Ha^2}{Re_L}, Ha^2 = \frac{\sigma B_0^2 L^2}{\mu},$$

$$Re_L = \frac{\Omega L^2 \sin\alpha}{\nu}, \Lambda = \frac{Gr_L}{Re_L^2},$$

$$Gr_L = \frac{g_c \beta_T (T_w - T_\infty) L^3}{\nu^2}, \Gamma = \frac{\beta_C (C_w - C_\infty)}{\beta_T (T_w - T_\infty)}, \tag{10}$$

2.2. Heat transfer analysis

The boundary layer energy equation in the presence of nonlinear thermal radiation and Dufour effect is given by:

$$u \frac{\partial T}{\partial x} + w \frac{\partial T}{\partial z} = (k_e / \rho c_p) \frac{\partial^2 T}{\partial z^2} + \frac{16\sigma^*}{3k_e^* \rho c_p} \frac{\partial}{\partial z} \left(T^3 \frac{\partial T}{\partial z} \right) + \frac{D_m k_T}{c_s c_p} \frac{\partial^2 C}{\partial z^2}, \tag{11}$$

with the boundary conditions:

$$-k \frac{\partial T}{\partial z} = h_1 (T_w - T), \text{ at } z = 0, \tag{12}$$

$$T = T_\infty, \text{ as } z \rightarrow \infty,$$

where T is the fluid temperature, T_w and T_∞ are the temperature of the fluid near the surface and ambient, respectively, c_p is the specific heat at constant pressure, σ^* is the Stefan-Boltzmann constant, k_e^* is the Rosseland mean absorption coefficient, k_e is the effective thermal conductivity of the fluid, c_s is the concentration susceptibility, D_m is the coefficient of mass diffusivity, k_T is the thermal diffusion ratio, h_1 is the convective heat transfer coefficient, and C is the concentration of the fluid. Using similarity transforms of (5), Eq. (11) reduced to:

$$\frac{1}{Pr} \left[\left(1 + Ra(1 + (\theta_w - 1)\theta)^3 \right) \theta' \right]' - \left(h\theta' - \frac{1}{2}h'\theta \right) + Du\phi'' = 0, \tag{13}$$

With the transformed boundary conditions:

$$\theta'(0) = -(1 - Bi_1(1 - \theta(0))),$$

$$\text{and } \theta(\infty) \rightarrow 0, \tag{14}$$

where Pr is the Prandtl number, Ra is the thermal radiation parameter, Bi_1 is the Biot number, and Du is the Dufour number, which are given by:

$$Pr = \frac{k_e}{\mu C_p}, Ra = \frac{16\sigma^* T_\infty^3}{3k_e k_e^*}, Bi_1 = \frac{h_1}{k} \sqrt{\frac{\nu}{a}},$$

$$Du = \frac{D_m k_T (C_L - C_\infty)}{c_s c_p \nu (T_L - T_\infty)}, \tag{15}$$

2.3. Mass transfer analysis

The boundary layer equation for conservation of mass in the presence of Soret effect is given by:

$$u \frac{\partial C}{\partial x} + w \frac{\partial C}{\partial z} = D_m \frac{\partial^2 C}{\partial z^2} + \frac{D_m k_T}{T_m} \frac{\partial^2 T}{\partial z^2}, \quad (16)$$

$$u \frac{\partial N}{\partial x} + w \frac{\partial N}{\partial z} = D_n \frac{\partial^2 N}{\partial z^2} - \frac{\partial(N\tilde{v})}{\partial z}, \quad (17)$$

The corresponding boundary conditions are:

$$\begin{aligned} -D_m \frac{\partial C}{\partial z} &= h_2 (C_w - C), N = N_w(x) \quad \text{at } z = 0, \\ C = C_\infty, N = N_\infty \quad \text{as } z \rightarrow \infty, \end{aligned} \quad (18)$$

where D_m is the coefficient of mass diffusivity, C is the concentration of the fluid, C_w and C_∞ are the concentrations near the wall and ambient, respectively, T_m is the mean temperature of the fluid, $\tilde{v} = (bW_c / C_w - C_\infty) \nabla C$, b is the chemotaxis constant, W_c is the maximum cell swimming speed (the product bW_c is assumed to be constant), N is the number density of motile microorganisms, N_w and N_∞ are the uniform concentration of microorganisms near the surface and for away from the surface, respectively, h_2 is the convective mass transfer coefficient, and D_n is the diffusivity of microorganisms. Using similarity transforms of (5), Eqs. (16 and 17) reduced to:

$$\frac{1}{Sc} \phi'' - \left(h\phi' - \frac{1}{2} h' \phi \right) + Sr\theta'' = 0, \quad (19)$$

$$\frac{1}{Pe} \xi'' - \left(h\xi' - \frac{1}{2} h' \xi \right) - (\phi' \xi' + (\gamma + \xi)\phi'') = 0, \quad (20)$$

The corresponding boundary conditions are:

$$\begin{aligned} \phi'(0) &= -(1 - Bi_2 (1 - \phi(0))), \xi(0) = 1, \text{ and} \\ \phi(\infty) &\rightarrow 0, \xi(\infty) \rightarrow 0, \end{aligned} \quad (21)$$

where Sc is the Schmidt number, Sr is the Soret number, Bi_1 is the Biot number, Pe is the Peclet number, and γ is the dimensionless parameter, which are given by:

$$\begin{aligned} Sc &= \frac{\nu}{D_m}, Sr = \frac{D_m k_T (C_L - C_\infty)}{T_m \nu (T_L - T_\infty)}, Bi_1 = \frac{h_1}{k} \sqrt{\frac{\nu}{a}}, \\ Pe &= \frac{bW_c}{D_n}, \gamma = \frac{N_\infty}{N - N_\infty}, \end{aligned} \quad (22)$$

For physical quantities of interest, the friction factors along x, y directions, local Nusselt, Sherwood numbers, and the local density of motile microorganisms are given by:

$$C_{fx} Re^{1/2} = -h''(0), \quad (23)$$

$$Re^{1/2} C_{fy} = -(1/2)g'(0),$$

$$Re^{-1/2} Nu_x = -[1 + Ra\theta_w^3] \theta'(0),$$

$$Re^{-1/2} Sh_x = -\phi'(0), \quad (24)$$

$$Re^{-1/2} Nn_x = -\xi'(0).$$

Where $Re = x^2 \Omega \sin \alpha / \nu$ is the Reynolds number.

3. Results and discussion

The set of nonlinear coupled ordinary differential Eqs. (6), (7), (8), (13), (19), (20) subjected to the dimensionless boundary conditions Eqs. (9), (14) and (21) are solved numerically using Runge–Kutta and Newton’s methods [30]. For an illustration of the results, numerical values are plotted in Figs. 2–43 and the effect of the governing fluid dynamical flow parameters on tangential, circumferential and normal velocities, dimensionless temperature, concentration and concentration of motile microorganisms is discussed in detail. For numerical computations, the non-dimensional parameter values are considered as:

$$Sr = Du = \gamma = 0.1, Pe = 2, M = Sc = Ra = \Gamma = 1, \\ Da^{-1} = 0.5, Bi_1 = Bi_2 = 0.4, \theta_w = 1.1, \delta = 5, \Lambda = 15$$

These values are kept as common in entire study except the variations in respective figures and tables.

The effect of Hartmann number M on velocity, temperature and concentration profiles of the flow are plotted through Figs. 2-7. It is observed that increasing values of the magnetic field parameter diminishes the tangential and circumferential velocities and enhances the normal velocity which can be seen from Figs. 2-4. It is interesting to mention that there is no significant difference in the circumferential velocity of the flow over a rotating cone and plate. It is due to the fact that the magnetic field exerts a force, known as Lorentz force, which suppresses the tangential and normal velocities. It is found from Figs. 5-7 that the thermal and species boundary layer thicknesses increase with an increase in the magnetic field. This is due to an additional resistance induced by the magnetic field. Inside the thermal and solutal boundary layers, the dimensionless temperature and concentration increase with a magnetic field. Further, it is also observed a notable hike in the both temperature and concentration of the fluid flow over a rotating cone when compared with the flow over a rotating plate.

The impact of nonlinear thermal radiation on velocity, temperature, and concentration profiles is demonstrated through Figs. 8-12. It is observed from Figs. 8 and 9, that an increase in the thermal radiation parameter causes the tangential velocity profile to rise, but the normal velocity to diminish. From Figs. 10-12, it is noticed that larger radiation parameter corresponds to an increase in the temperature field whereas the opposite trend for the dimensionless concentration. Physically, an increase in the radiation parameter provides more heat to the fluid that depicts an enhancement in the temperature and thermal boundary layer thickness. It is worthy to mention that there is a significant difference in the dimensionless temperature and concentration of the flow over a rotating cone and plate.

The variations in velocity, temperature, and concentration corresponding to the various

values of Biot numbers Bi_1 and Bi_2 are studied in Figs. 13–21. It can be concluded from Figs. 13 & 17 that the tangential velocity is lower for the larger values of Biot numbers Bi_1 and Bi_2 while the opposite behavior is observed for the normal velocity which is evident from Figs. 14 & 18. Figures. 15 and 19 elucidate that the larger values of Biot number Bi_1 tends to reduce the dimensionless temperature and thermal boundary layer thickness whereas gives reverse effect for the Biot number Bi_2 . It is seen that the Biot numbers Bi_1 and Bi_2 have the opposite trend in the temperature and concentration (see Figs. 16 and 20). Figure 21 shows the effects of the Biot number Bi_2 on the dimensionless density of motile microorganisms. It is observed that the dimensionless density of motile microorganisms increases for rising values of the Biot number Bi_2 . Further, it is also interesting to note that there is no significant difference in the circumferential velocity of the flow over a rotating cone and plate due to variation in the Biot numbers.

The influence of porosity parameter δ on velocity, temperature, and concentration fields is displayed in Figs. 22-27. It is indicated that an increase in the porosity parameter δ causes a significant decrease in the peaks of normal velocity and circumferential velocity, dimensionless temperature and concentration fields whereas the opposite behavior to the tangential velocity. This is due to the fact that the presence of a porous medium in the flow develops the resistance to the flow, thus, this resistive force tends to slow the motion of the fluid along the rotating cone and plate and causes a decrease in its temperature and concentration. The effect of γ on the concentration of motile microorganisms is presented in Fig. 28. It is noticed that an increase in γ results in depreciation in the concentration of motile microorganisms.

Figures 29-33 demonstrates the impact of Soret number Sr on velocity, temperature and concentration distributions. It is evident from Figs. 29 & 30 that an increase in the Soret

parameter enhances the velocity profiles at the tangential direction and diminishes the velocity profile in the normal direction. Physically, increasing values of Soret parameter boots the thermal boundary layer thickness; this helps to develop the tangential momentum boundary layer thickness. From Fig. 31, it is observed that the temperature diminishes with an increase in the Soret parameter while the opposite trend to the concentration and concentration of motile microorganisms of the flow (see Figs. 32 and 33). Also, Soret parameter has a tendency to strengthen the boundary layer thickness of temperature. Figures 34-38 display the typical profiles of the dimensionless velocity, temperature, and concentration for different values of Dufour number. An increase in the Dufour number enhances the dimensionless temperature, as displayed in Fig. 36, whereas it diminishes the concentration profiles of the flow, as displayed in Figs. 37 and 38. This is due to fact that the relationship between Soret number and Dufour numbers are in which the product is a constant.

The impact of buoyancy parameter Λ on velocity, temperature, and concentration fields is depicted through Figs. 39-43. From Figs.39 & 40 it can be observed that increasing values of the buoyancy parameter results in enhancement oftangential velocity profiles while it suppresses the normal velocity along with the thermal and concentration boundary layers. The buoyancy parameter is the ratio of the buoyancy to the viscous forces; this accelerates the fluid and works as a pressure gradient. In the presence of buoyancy forces, the viscous forces are negligible. This may be the reason for the reduction in the temperature and concentration profiles of the flow (see Figs.41-43).

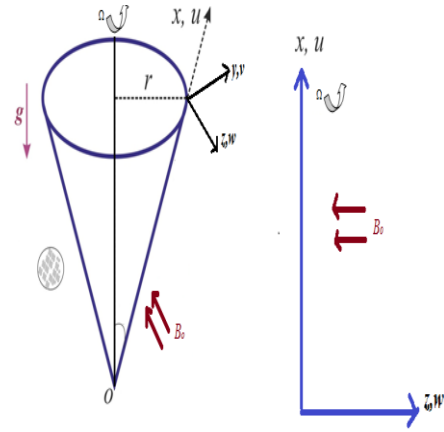


Fig. 1. Geometry of the problem.

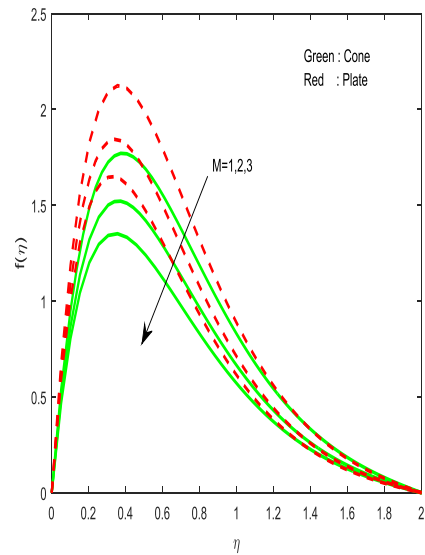


Fig. 2. Variations of the Hartmann number M on tangential velocity.

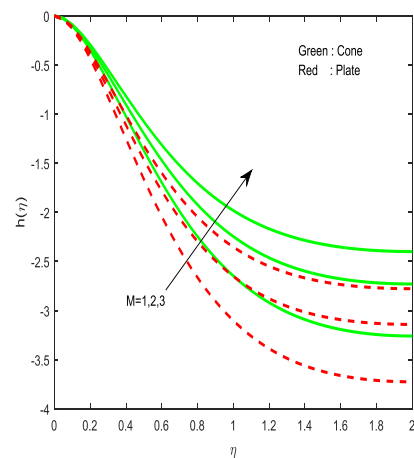


Fig. 3. Variations of the Hartmann number M on normal velocity.

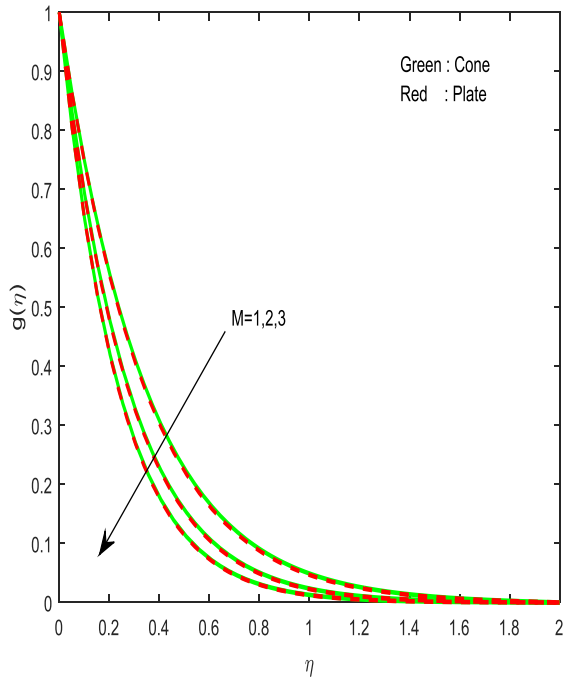


Fig. 4. Variations of the Hartmann number M on circumferential velocity.

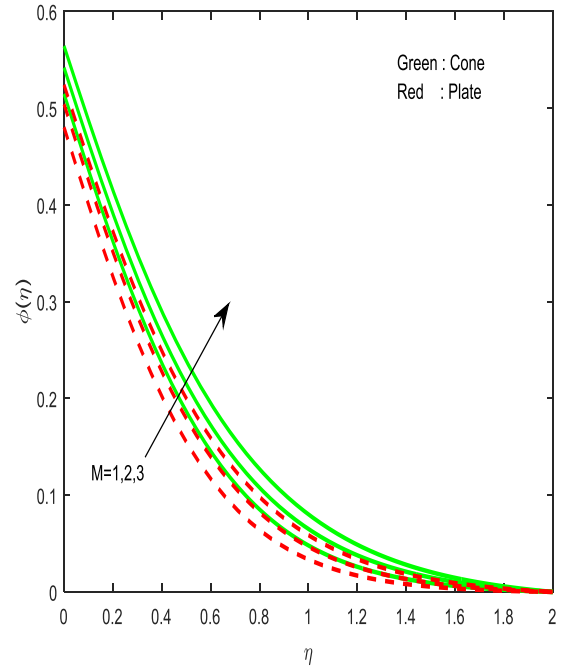


Fig. 6. Variations of Hartmann number M on dimensionless concentration.

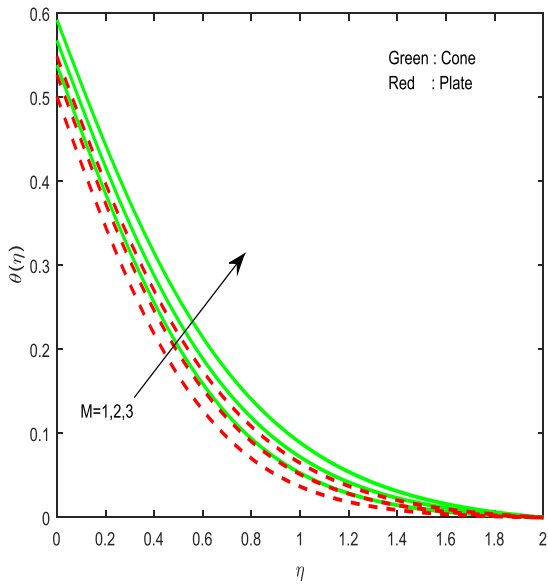


Fig. 5. Variations of Hartmann number M on dimensionless temperature.

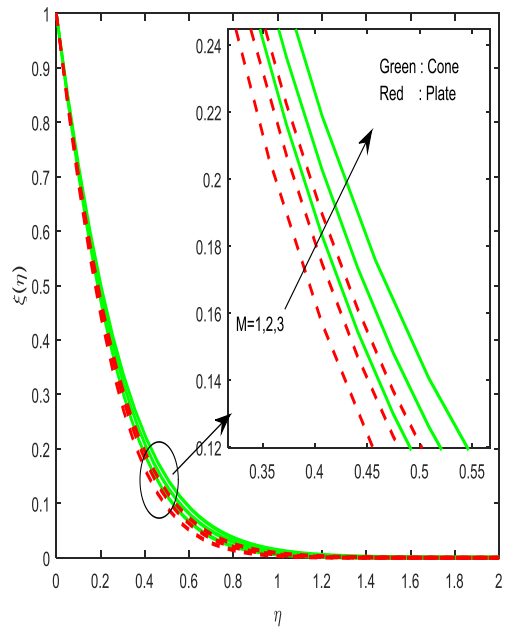


Fig. 7. Variations of Hartmann number M on concentration of motile microorganisms.

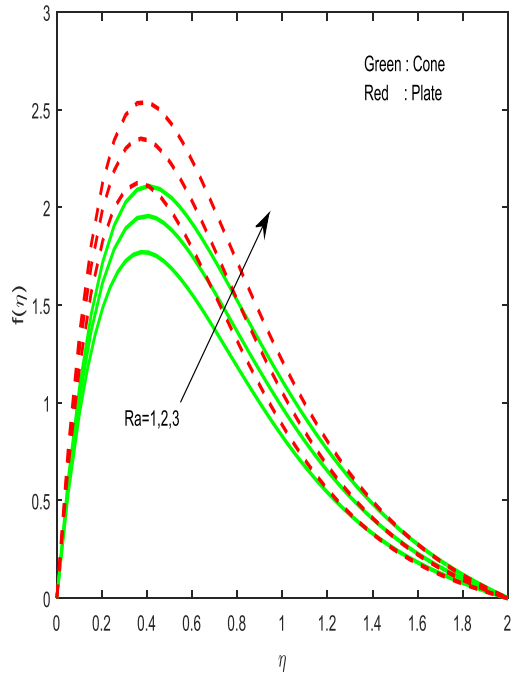


Fig. 8. Variations of the radiation parameter Ra on tangential velocity.

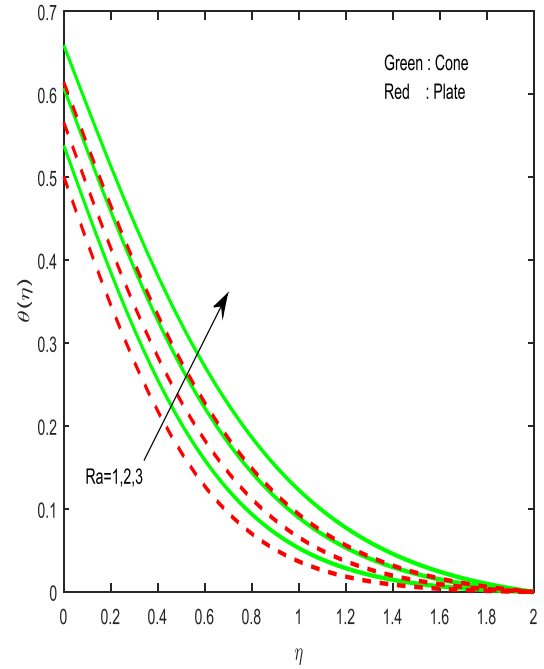


Fig. 10. Variations of radiation parameter Ra on dimensionless temperature.

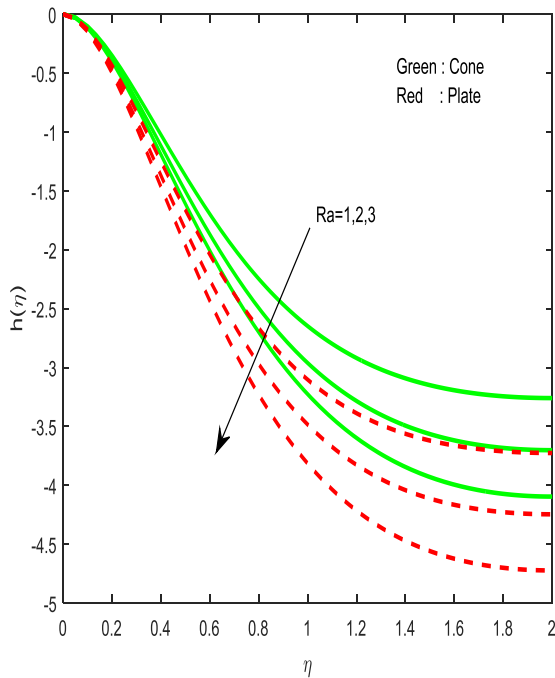


Fig. 9. Variations of the radiation parameter Ra on normal velocity.

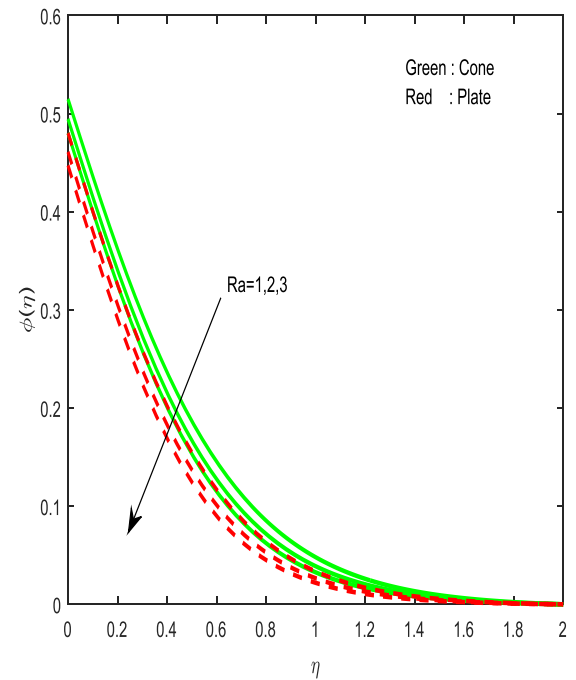


Fig. 11. Variations of radiation parameter Ra on dimensionless concentration.

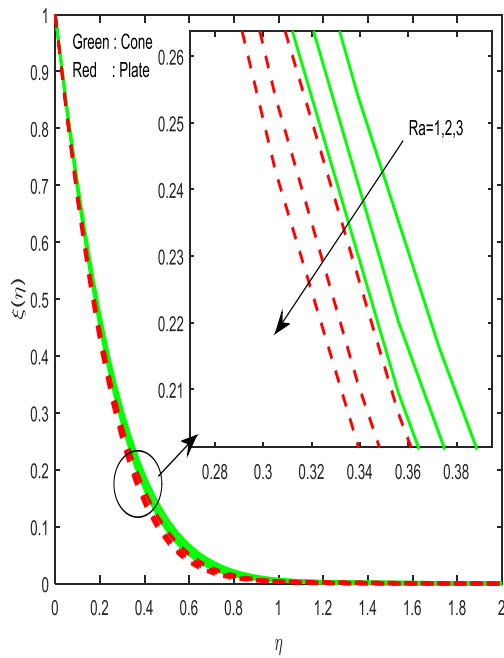


Fig. 12. Variations of radiation parameter Ra on concentration of motile microorganisms.

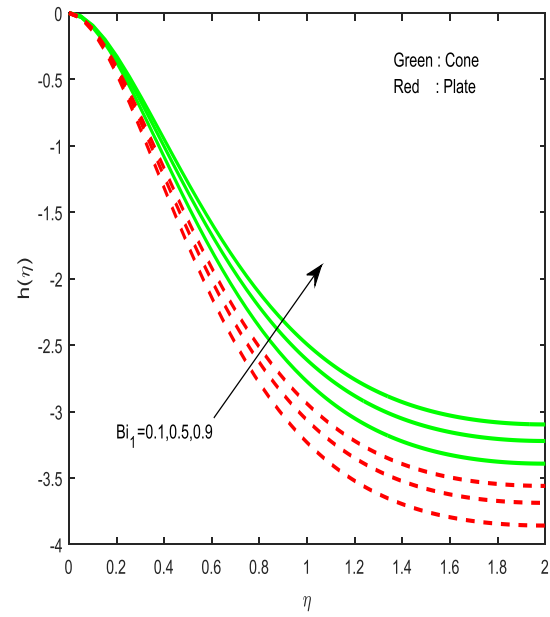


Fig. 14. Variations of Biot number Bi_1 on normal velocity.

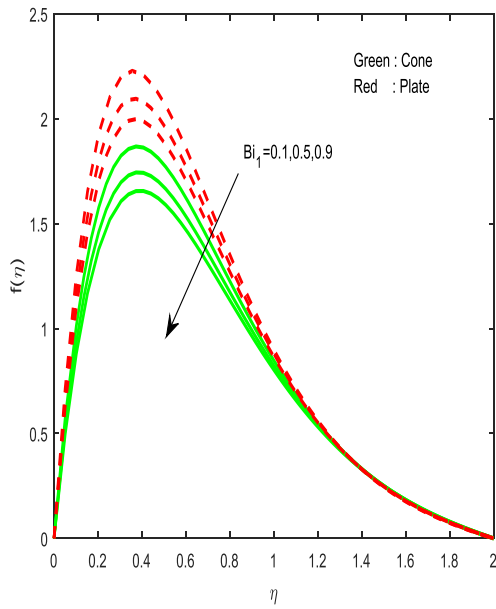


Fig. 13. Variations of Biot number Bi_1 on tangential velocity.

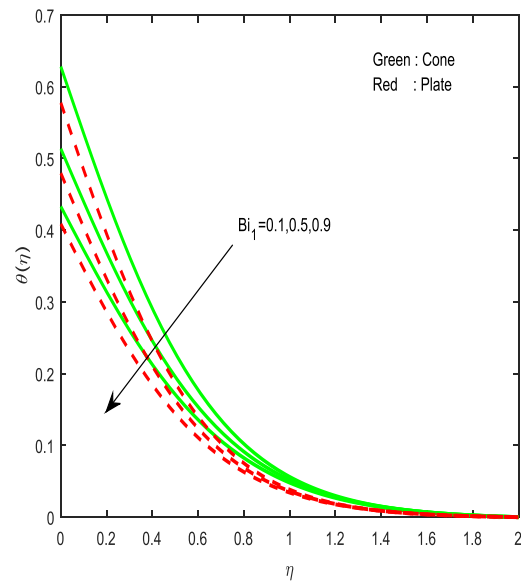


Fig. 15. Variations of Biot number Bi_1 on dimensionless temperature.

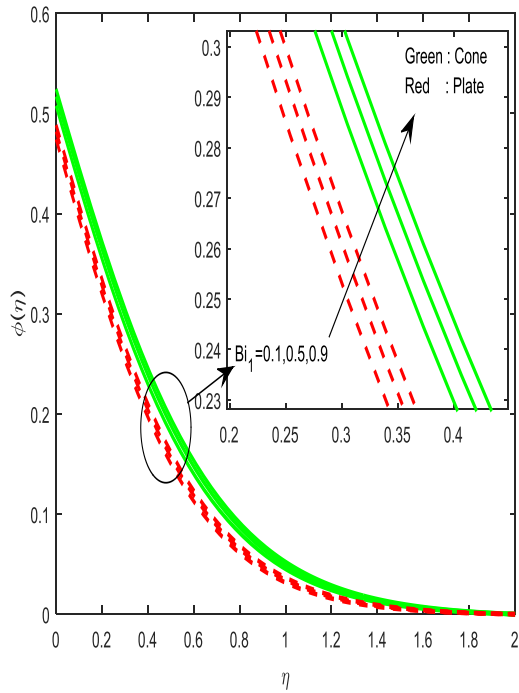


Fig. 16. Variations of Biot number Bi_1 on dimensionless concentration.

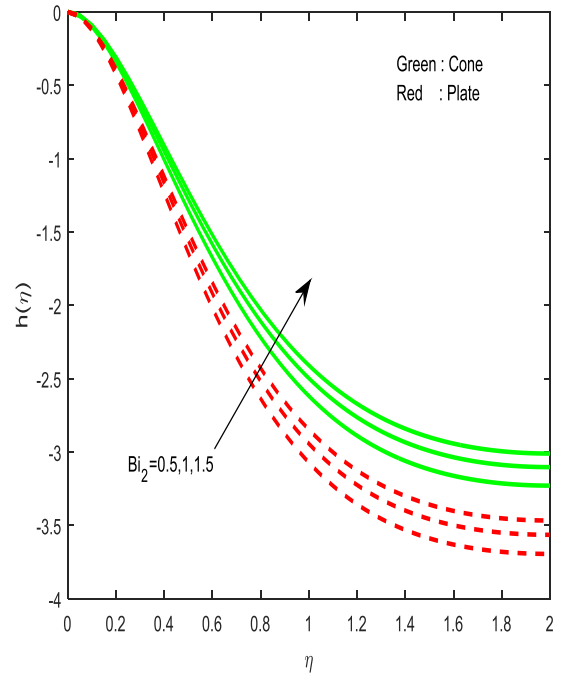


Fig. 18. Variations of Biot number Bi_2 on normal velocity.

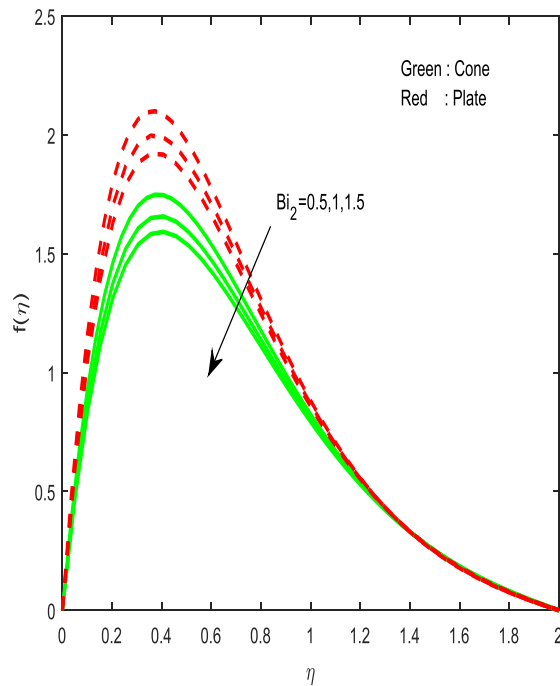


Fig. 17. Variations of Biot number Bi_2 on tangential velocity.

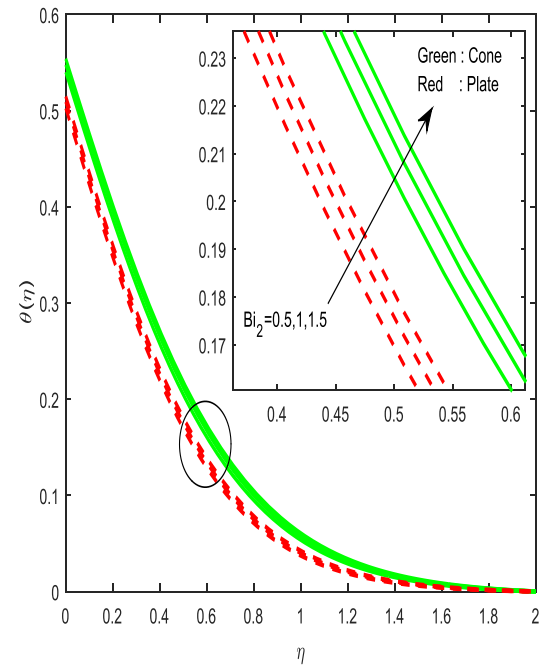


Fig. 19. Variations of Biot number Bi_2 on dimensionless temperature.

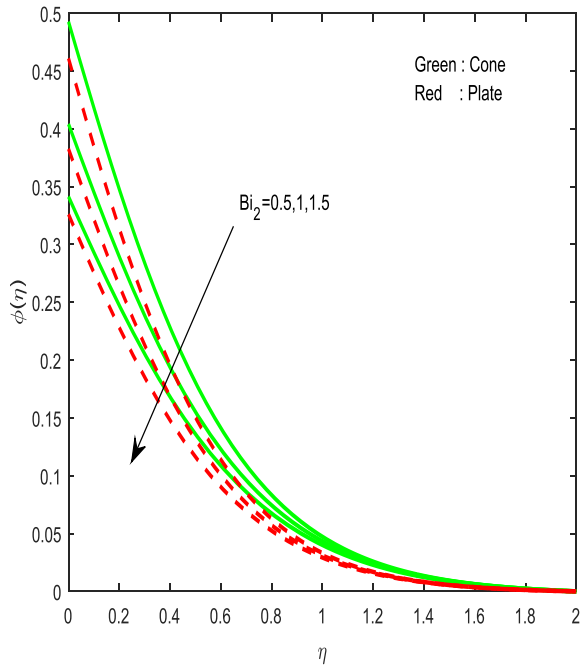


Fig. 20. Variations of Biot number Bi_2 on dimensionless concentration.

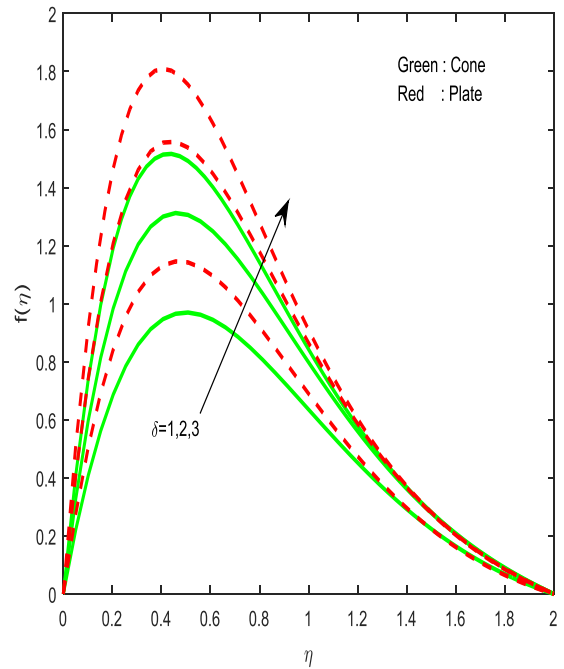


Fig. 22. Variations of the porosity parameter δ on tangential velocity.

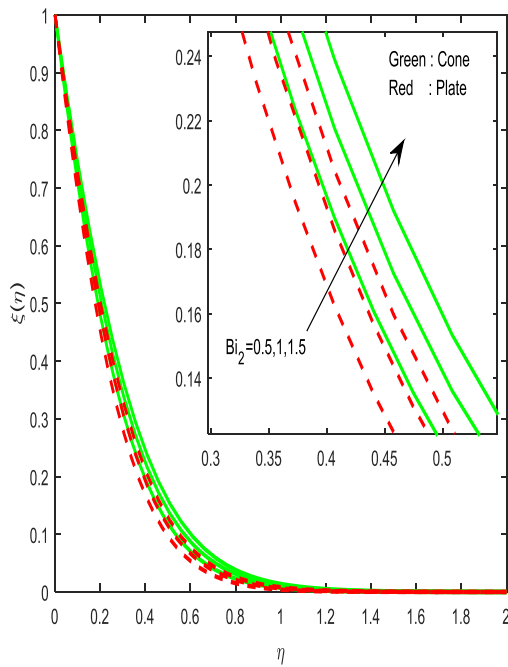


Fig. 21. Variations of Biot number Bi_2 on concentration of motile microorganisms.

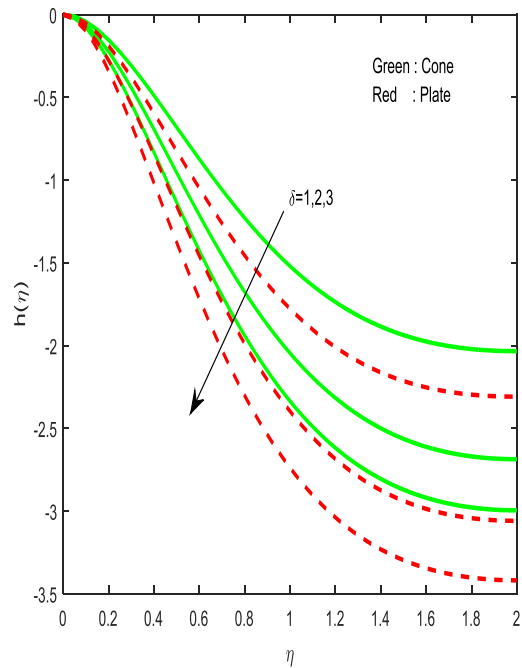


Fig. 23. Variations of the porosity parameter δ on normal velocity.

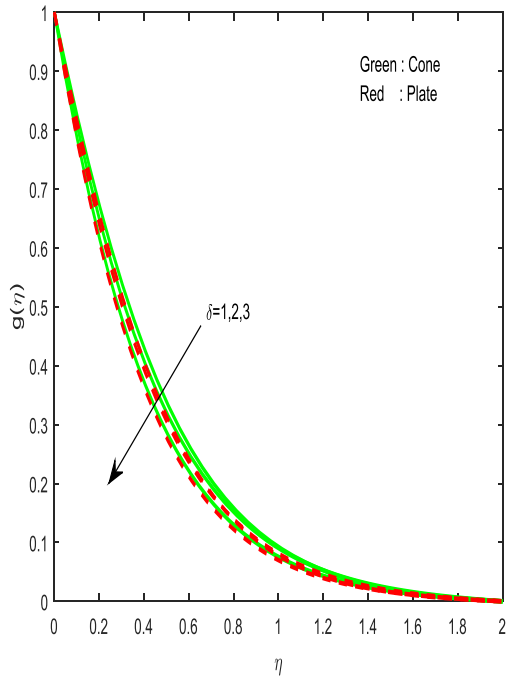


Fig. 24. Variations of the porosity parameter δ on circumferential velocity.

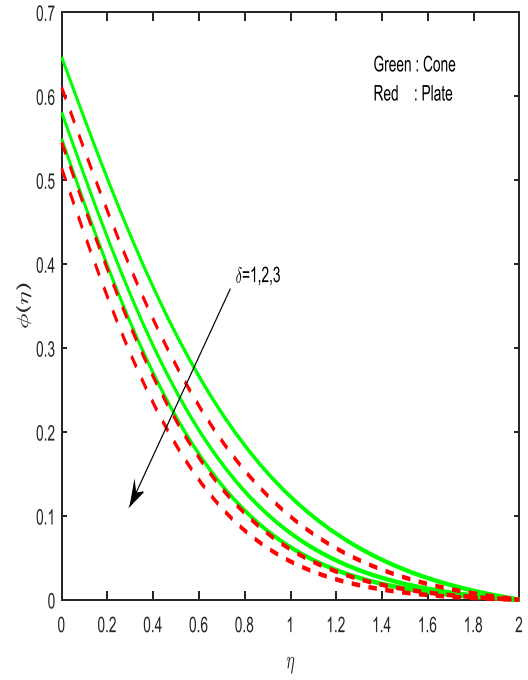


Fig. 26. Variations of the porosity parameter δ on dimensionless concentration.

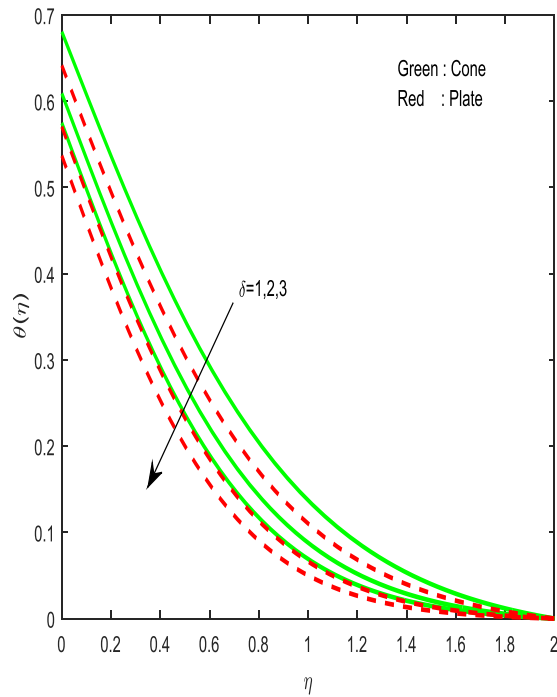


Fig. 25. Variations of the porosity parameter δ on dimensionless temperature.

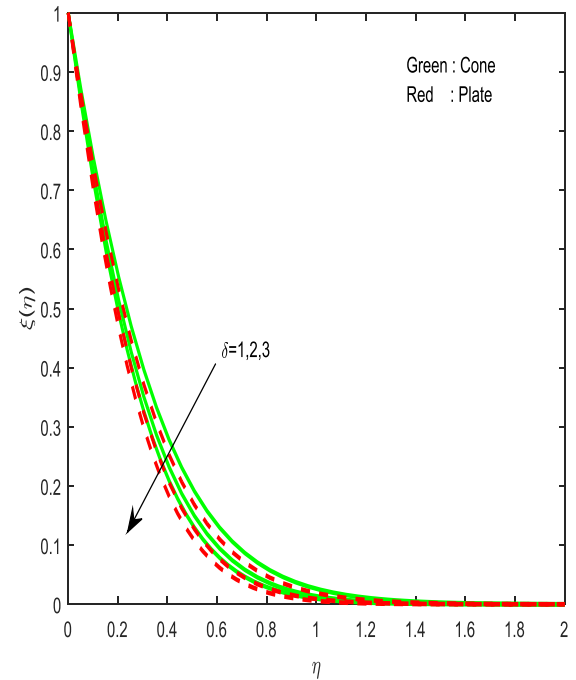


Fig. 27. Variations of the porosity parameter δ on concentration of motile microorganisms.

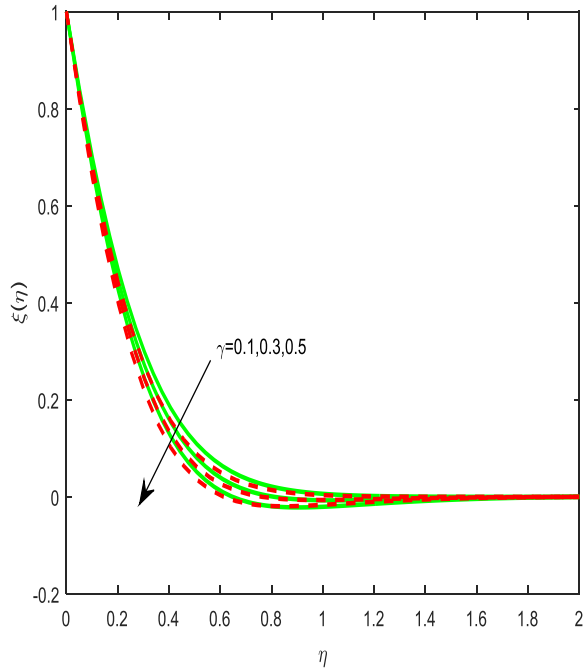


Fig. 28. Variations of γ on the concentration of motile microorganisms.

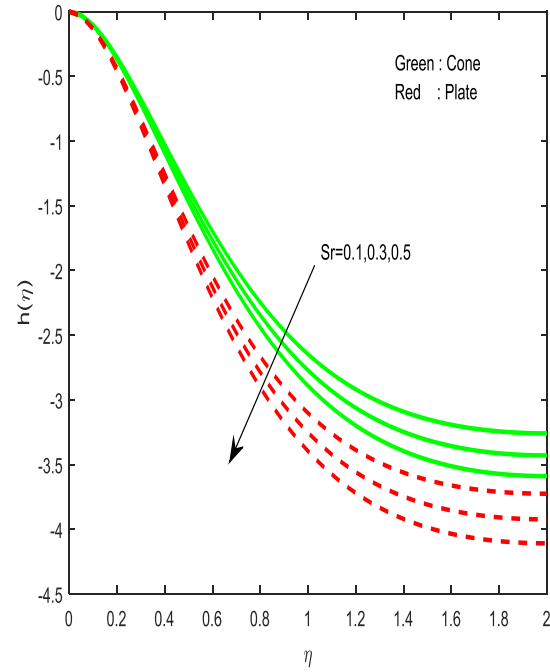


Fig. 30. Variations of the Soret number Sr on normal velocity.

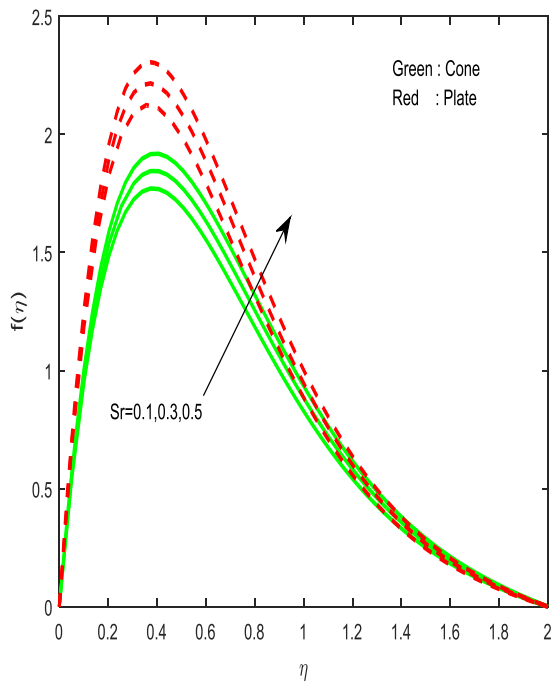


Fig. 29. Variations of the Soret number Sr on tangential velocity.

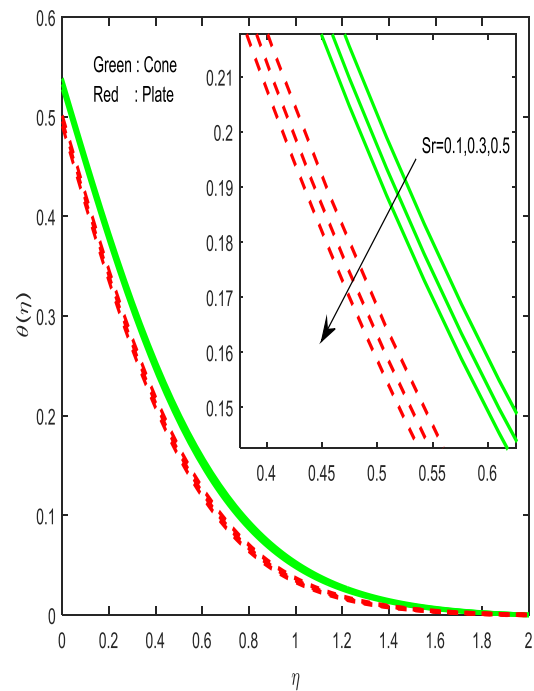


Fig. 31. Variations of the Soret number Sr on dimensionless temperature.

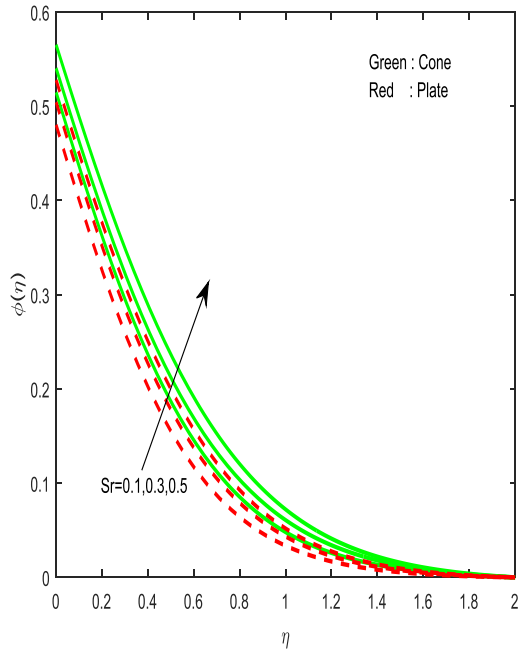


Fig. 32. Variations of the Soret number Sr on dimensionless concentration.

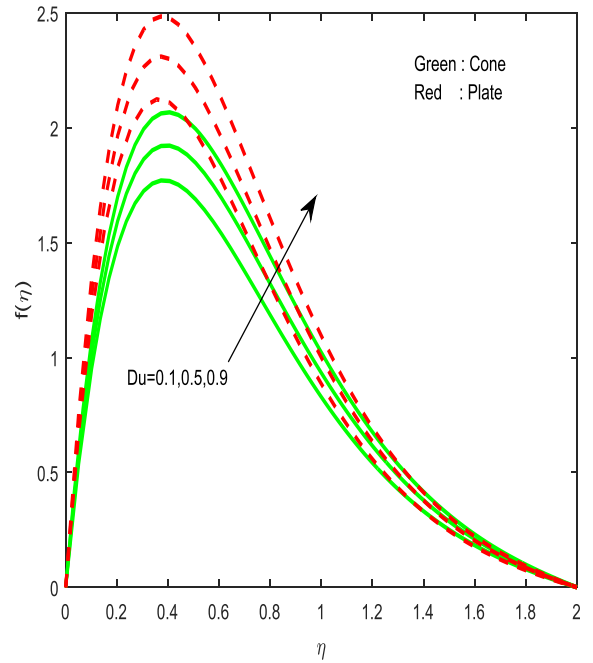


Fig. 34. Variations of the Dufour number Du on tangential velocity.

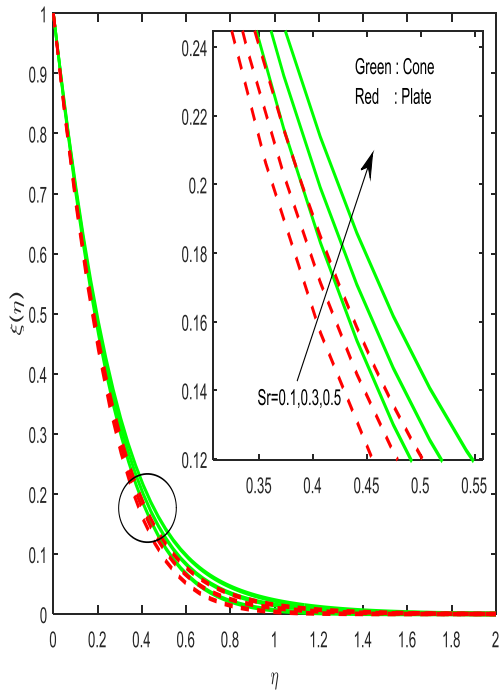


Fig. 33. Variations of the Soret number Sr on concentration of motile microorganisms.

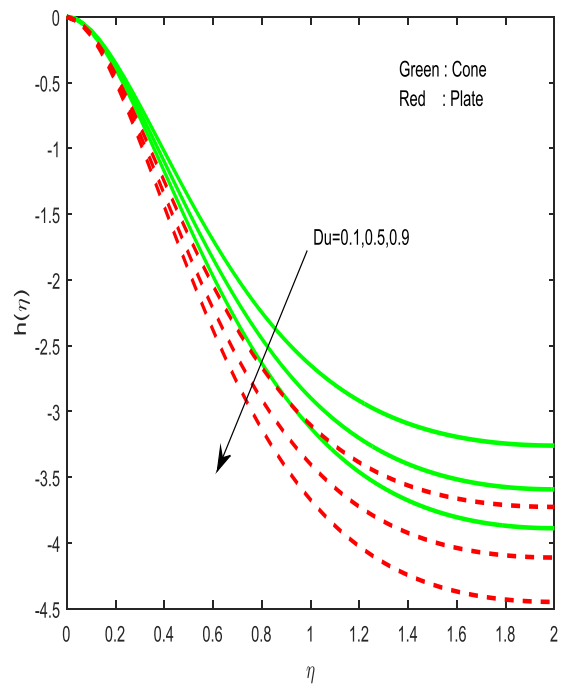


Fig. 35. Variations of the Dufour number Du on tangential velocity.

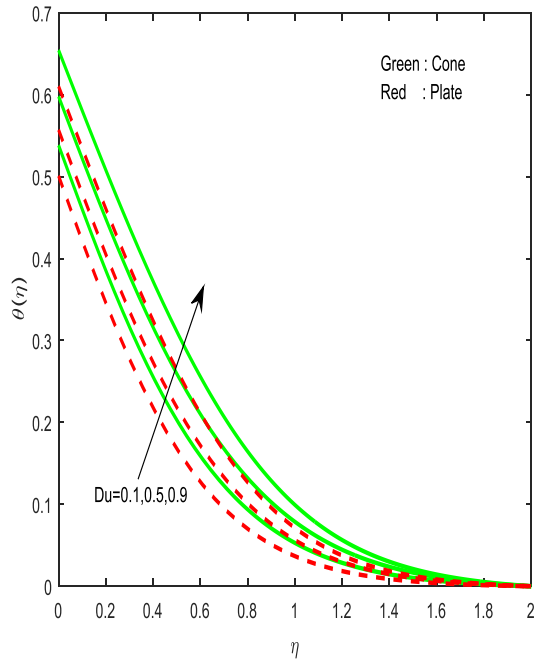


Fig. 36. Variations of the Dufour number Du on dimensionless temperature.

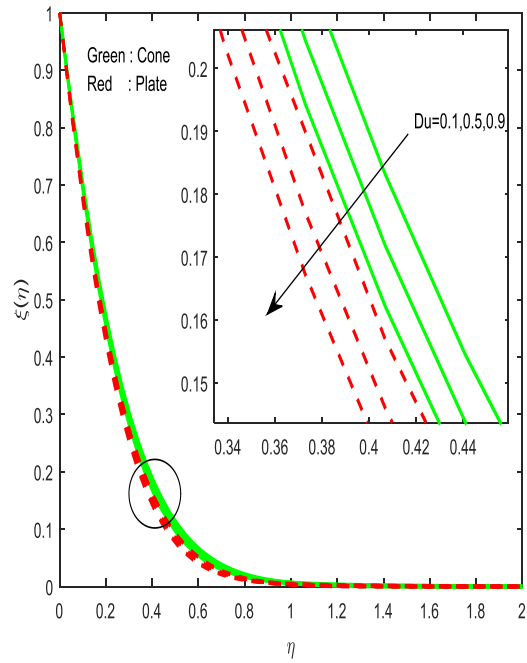


Fig. 38. Variations of the Dufour number Du on concentration of motile microorganisms.

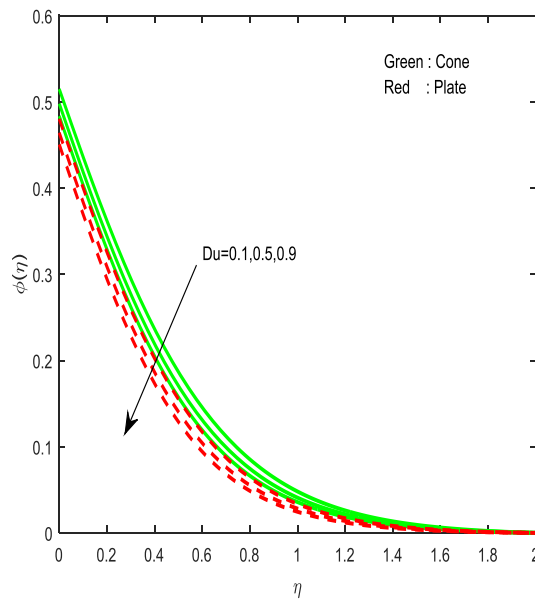


Fig. 37. Variations of the Dufour number Du on dimensionless concentration.

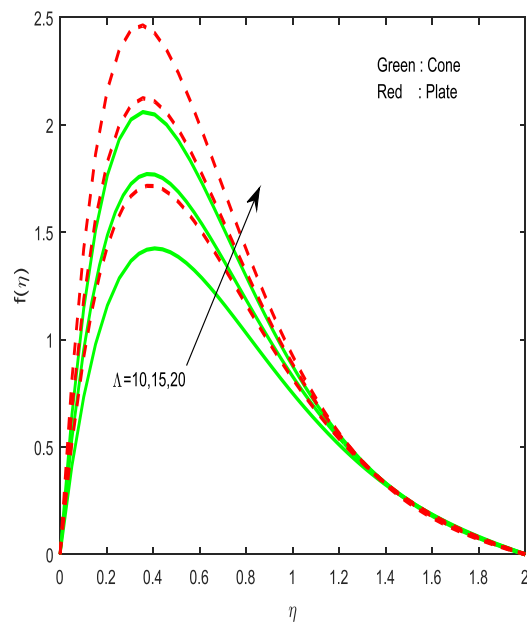


Fig. 39. Variations of the buoyancy parameter Λ on tangential velocity.

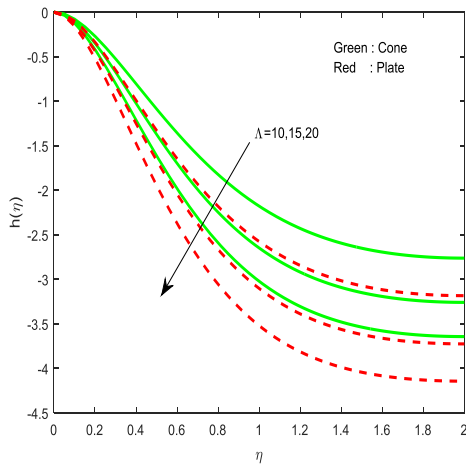


Fig. 40. Variations of the buoyancy parameter Λ on normal velocity.

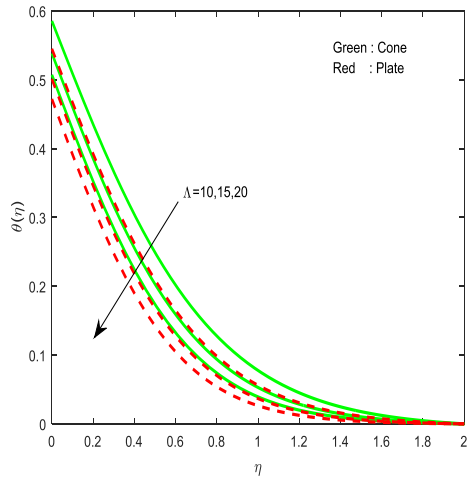


Fig. 41. Variations of the buoyancy parameter Λ on the dimensionless temperature.

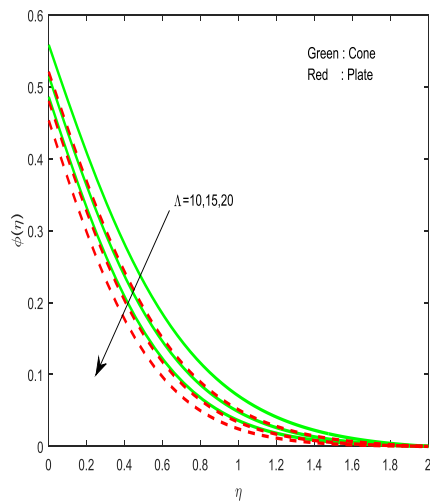


Fig. 42. Variations of the buoyancy parameter Λ on the dimensionless concentration.

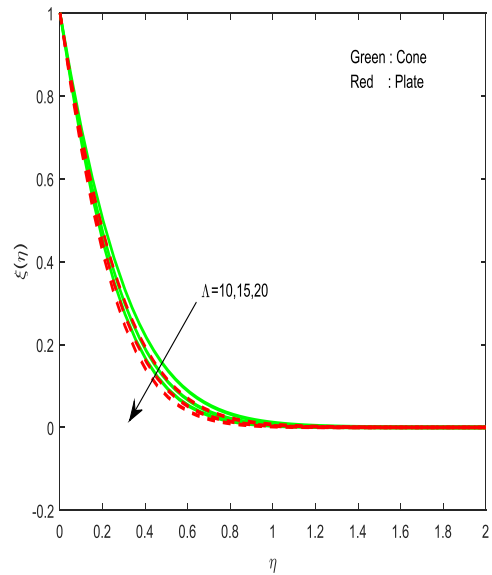


Fig. 43. Variations of the buoyancy parameter Λ on concentration of motile microorganisms.

The numerical values of dimensionless skin friction coefficients, local Nusselt and Sherwood numbers for various parametric values of Hartmann number M , radiation parameter Ra , porosity parameter δ , buoyancy parameter Λ , Biot numbers Bi_1 and Bi_2 are given in Table 1. It is observed that skin friction coefficient along tangential direction diminishes with an increase in Hartmann number M while it enhances in the normal direction. Both heat and mass transfer rates are depreciated with increasing the magnetic field over a rotating cone and plate. It is found that increasing values of the radiation parameter causes the heat transfer rate to fall while the opposite effect to the mass transfer rate. The friction factors, heat and mass transfer rates increase for higher values of porosity parameter and buoyancy parameter whereas the reverse trend to the Biot numbers Bi_1, Bi_2 . Validation of the present results for friction factor and local Nusselt number by comparing with the published results are presented in Table 2. It proves the validity and accuracy of the present results.

Table 1. Variation in friction fact, local Nusselt and Sherwood numbers for different dynamical values of non-dimensional governing parameters.

	M	Ra	δ	Λ	Bi_1	Bi_1	$-h''(0)$	$-g'(0)$	$-\theta'(0)$	$-\phi'(0)$	$-\xi'(0)$
Cone	1						23.87450	2.848490	0.784668	0.794058	3.254832
	2						22.36767	3.604685	0.772877	0.783260	3.137426
	3						21.26219	4.233023	0.763087	0.774316	3.044669
Plate	1						30.10262	2.871995	0.799602	0.807901	3.459578
	2						28.34034	3.620720	0.789211	0.798350	3.343566
	3						27.03456	4.245111	0.780483	0.790350	3.251241
Cone	1						23.87450	2.848490	0.784668	0.794058	3.254832
	2						25.62299	2.858244	0.756868	0.802171	3.348032
	3						26.99169	2.866046	0.736333	0.807900	3.417576
Plate	1						30.10262	2.871995	0.799602	0.807901	3.459578
	2						32.34707	2.884093	0.773527	0.815602	3.559550
	3						34.12924	2.893933	0.754090	0.821092	3.635229
Cone			1				9.474636	1.812639	0.727746	0.741521	2.631144
			2				14.19187	2.047875	0.756348	0.767822	2.903186
			3				17.90521	2.324497	0.770051	0.780488	3.059774
Plate			1				11.83680	1.901540	0.743394	0.755920	2.778186
			2				17.82423	2.105253	0.771748	0.782036	3.073948
			3				22.53260	2.364702	0.785240	0.794535	3.245190
Cone				10			18.14872	2.825593	0.765857	0.776683	3.029319
				15			23.87450	2.848490	0.784668	0.794058	3.254832
				20			28.94434	2.867720	0.797138	0.805613	3.423958
Plate				10			22.94725	2.844873	0.782026	0.791614	3.221174
				15			30.10262	2.871995	0.799602	0.807901	3.459578
				20			36.43275	2.894675	0.811217	0.818701	3.638744
Cone					0.1		25.48454	2.854802	0.937189	0.796915	3.302287
					0.5		23.43033	2.846735	0.743211	0.793218	3.241282
					0.9		21.98450	2.840978	0.610273	0.790305	3.195665
Plate					0.1		31.94587	2.878828	0.942236	0.810329	3.506231
					0.5		29.58645	2.870066	0.760225	0.807179	3.446102
					0.9		27.88226	2.863647	0.632091	0.804647	3.400216
Cone					0.5		23.48743	2.846993	0.783957	0.753640	3.182202
					1		21.93610	2.840936	0.780873	0.595838	2.898962
					1.5		20.83434	2.836578	0.778433	0.487926	2.705356
Plate					0.5		29.64988	2.870338	0.798985	0.769520	3.390455
					1		27.80958	2.863540	0.796283	0.617293	3.116354
					1.5		26.47576	2.858547	0.794111	0.510833	2.924495

Table 2 Validation in the present results for skin friction coefficient and local Nusselt number when $Pr = 0.7, Da^{-1} = \Gamma = Sr = Du = Sc = Pe = \gamma = 0$.

Λ	Mallikarjuna et al. [27] $-g'(0)$	Present Results $-g'(0)$	Mallikarjuna et al. [27] $-\theta'(0)$	Present Results $-\theta'(0)$
0	0.61583	0.615831	0.42842	0.428422
0.1	0.65492	0.654924	0.46141	0.461411
1.0	0.85080	0.850800	0.61213	0.612123
10	1.40363	1.403631	1.01748	1.017480

4. Conclusions

In this study, a mathematical model was presented to explore the characteristics of the magnetohydrodynamic free convective heat and mass transfer of the flow past a permeable vertical rotating cone and plate filled with gyrotactic microorganisms in the presence of nonlinear thermal radiation, thermo diffusion and diffusion thermo effects. The numerical findings are as follows:

- The rate of heat and mass transfer is high on the flow through rotating plate when compared with the rotating cone.
- The heat and mass transfer performance of the flow over a cone is significantly high when compared with the flow over a plate.
- There is no significant variation in the circumferential velocity filed on the flow over a cone and a plate.
- Porosity parameter has a tendency to enhance the heat and mass transfer rate.
- Biot numbers act like regulating parameters of heat and mass transfer.
- Soret and Dufour numbers help to control the thermal and concentration boundary layers.

References

[1] M. AboeldahabEmad, “Radiation effect on heat transfer in electrically conducting fluid at a stretching surface with uniform free stream”, *J. Phys D App. Phys.*, Vol. 33, No. 24, pp. 3180–3185, (2000).

[2] M. Gnaneswara Reddy, “Influence of magnetohydrodynamic and thermal radiation boundary layer flow of a nanofluid past a stretching sheet”, *Journal of Scientific Research*, Vol. 6, No. 2, pp. 257-272 (2014).

[3] E. M. Abo-Eldahab, and M. S. Elgendy, “Radiation effect on convective heat transfer in an electrically conducting fluid at a stretching surface with variable viscosity and uniform free stream”, *Physica Scripta*, Vol. 62, No. , pp. 321-325, (2000).

[4] A. Aziz, “A similarity solution for laminar thermal boundary layer over a flat plate with a convective surface boundary condition”, *Communications in Nonlinear Science and Numerical Simulation*, Vol. 14, No. 4, pp. 1064-068, (2009).

[5] R. Cortell, “Radiation effects for the Blasius and Sakiadis flows with a convective surface boundary condition”, *Applied Mathematics and Computation*, Vol. 206, No.1, pp. 832-840, (2008).

[6] A. Ishak, “Similarity solutions for flow and heat transfer over a permeable surface with convective boundary condition”, *Appl Math Comput*, Vol. 217, No. 2, pp. 837-842, (2010).

[7] S. Yao, T. Fang and Y. Zhong, “Heat transfer of a generalized stretching/shrinking wall problem with convective boundary conditions”, *Comm Nonlinear SciNumSimul*, Vol. 16, No. 2, pp. 752-760, (2011).

[8] A. Alsaedi, Z. Iqbal, M. Mustafa, T. Hayat, “Exact solutions for the magnetohydrodynamic flow of a Jeffrey fluid with convective boundary conditions and chemical reaction”, *Z Naturforsch*, Vol. 67a, No. 1, pp. 517- 524, (2012).

[9] O. D. Makinde, and A. Aziz, “Boundary layer flow of a nanofluid past a stretching sheet with a convective boundary

- condition”, *Int. J. Therm Sci.*, Vol. 50, No.7, pp. 1326-1332, (2011).
- [10] M. Gnaneswara Reddy, “Thermal radiation and chemical reaction effects on MHD mixed convective boundary layer slip flow in a porous medium with heat source and Ohmic heating”, *Eur. Phys. J. Plus*, Vol. 129, No. 41, pp.1-17, (2014).
- [11] M. Gnaneswara Reddy, “Effects of Thermophoresis, viscous dissipation and Joule heating on steady MHD flow over an inclined radiative isothermal permeable surface with variable thermal conductivity”, *Journal of Applied Fluid Mechanics*, Vol. 7, No. 1, pp. 51-61, (2014).
- [12] A. Bejan, *Convection Heat Transfer*, 3rd edn. Wiley, New York (2013)
- [13] A. Bejan, and R. K. Khair, “Heat and mass transfer by natural convection in a porous medium”, *Int. J. Heat Mass Transfer*, Vol. 28, pp. 909–918, (1985).
- [14] D. A. Nield, and A. Bejan, *Convection in Porous Media*, 4th edn. Springer, New York (2013)
- [15] I. Pop, and D. B. Ingham, *Convective Heat Transfer: Mathematical and Computational Modeling of Viscous Fluids and Porous Media*, Pergamon, Oxford (2001)
- [16] D. B. Ingham, and I. Pop, *Transport Phenomena in Porous Media II*, Pergamon, Oxford (2002)
- [17] E.M. Sparrow, and J. L. Gregg, “Mass transfer, flow and heat transfer about a rotating disk”, *Trans. Am. Soc. Mech. Eng. Ser. C J. Heat Transfer*, Vol. 82, No. 4, pp. 294–302, (1960).
- [18] R. G. Hering, and R. J. Grosh, “Laminar free convection from a non-isothermal cone at low Prandtl number”, *Int. J. Heat Mass Transfer*, Vol. 8, No. 10, pp. 1333–1337, (1965).
- [19] F. Kreith, “Convective heat transfer in rotating systems “, *In: Irvine, T.F., Hamett, J.P. (eds.) Advances in Heat Transfer*, Vol. 5, pp. 129–251, (1968).
- [20] K. Himasekhar, P.K. Sarma, and K. Janardhan, “Laminar mixed convection from a vertical rotating cone”, *Int. Commun. Heat Mass Transfer*, Vol. 16, No. 1, pp. 99–106, (1989).
- [21] A.J. Chamkha, “Combined convection heat transfer from a rotating cone embedded in a power-law fluid saturated porous medium”, *Fluid/Particle Separat. J.*, Vol. 13, No. 1, pp. 12–29, (2000).
- [22] H.S. Takhar, A.J. Chamkha, and G. Nath, “Unsteady mixed convection flow from a rotating vertical cone with a magnetic field”, *Heat Mass Transfer*, Vol. 39, No. 4, pp. 297–304, (2003)
- [23] S. Roy, and D. Anil kumar, “Unsteady mixed convection from a rotating cone in a rotating fluid due to the combined effects of thermal and mass diffusion”, *Int. J. Heat Mass Transfer*, Vol. 47, No. 8, pp. 1673–1684, (2004).
- [24] M. Gnaneswara Reddy, and N. Bhaskar Reddy, “Mass Transfer and heat generation effects on MHD free convection flow past an inclined vertical surface in a porous medium”, *Journal of Applied Fluid Mechanics*, Vol. 4, No. 2, pp. 7-11, (2011).
- [25] R. Bhuvanavijaya, and B. Mallikarjuna,” Effect of variable thermal conductivity on convective heat and mass transfer over a vertical plate in a rotating system with variable porosity regime”, *J. Naval Architect. Mar. Eng.*, Vol. 11, pp. 83–92, (2014).
- [26] M. Gnaneswara Reddy, “Lie group analysis of heat and mass transfer effects on steady MHD free convection dissipative fluid flow past an inclined porous surface with heat generation”, *Theoret. Appl. Mech.*, Vol. 39, No. 3, pp. 233–254, (2012).
- [27] B. Mallikarjuna, A. M. Rashad, Ali J. Chamkha, and S. Hariprasad Raju, “Chemical reaction effects on MHD convective heat and mass transfer flow past a rotating vertical cone embedded in a variable porosity regime”, *AfrikaMathematika*, Vol. 27, pp. 645-665, (2016).
- [28] G. Awad, P. Sibanda, S.S. Mosta, and O.D. Makinde, “Convection from an

- inverted cone in a porous medium with cross-diffusion effects”, *Comp. Maths. Apps.*, Vol. 61, No. 5, pp. 1431–1441, (2011).
- [29] N. Sandeep, B. Rushi Kumar and M. S. Jagadeesh Kumar, “A comparative study on convective heat and mass transfer in non-Newtonian nano fluid flow past a permeable stretching sheet”, *J. Mol. Liq.* Vol. 212, pp. 585-591, (2015).
- [30] C.S.K. Raju, and N. Sandeep, Heat and mass transfer in MHD non-Newtonian bio-convection flow over a rotating cone/plate with cross diffusion, *Journal of Molecular Liquids*, Vol. 215, pp. 115-126, (2016).
- [31] M. Gnanaswara Reddy, and N. Sandeep, “Heat and mass transfer in radiative MHD Carreau fluid with cross diffusion”, *Ain Shams Engineering Journal*, (2016) (Article in Press).

How to cite this paper:

M. Gnanaswara Reddy, and N. Sandeep, “Free convective heat and mass transfer of magnetic bio-convective flow caused by a rotating cone and plate in the presence of nonlinear thermal radiation and cross diffusion”, *Journal of Computational and Applied Research in Mechanical Engineering*, Vol. 7. No. 1, pp. 1-21

DOI: 10.22061/JCARME.2017.641

URL: http://jcarme.srttu.edu/article_641.html

